Combination of SHE- and SHM-PWM Techniques for VSI DC-Link Current Harmonics Control in Railway Applications

Marcin Steczek, *Member, IEEE*, Piotr Chudzik, and Adam Szeląg

***Abstract*—The paper presents an innovative concept of applying a combination of well-known selective harmonic elimination (SHE) and selective harmonics mitigation (SHM) methods to shape a spectrum of catenary current harmonics, generated by a traction drive system equipped with a voltage source inverter. Application of this method allows for reducing distorting influence of a modern rolling stock supplied by a 3 kV dc catenary on the railway signaling, command, and control systems. The efficiency of the proposed method is independent of synchronization of a vehicle's inverters and of load balance of traction motors, which makes it more reliable than as it is proposed in the literature. Results of computer simulations were presented and compared with laboratory measurements. The obtained dc-link current spectrum using the proposed SHE/SHM method was compared with spectra received using synchronized and unsynchronized sinusoidal pulse-width modulations (SPWMs). Based on the conducted tests, it was shown that the proposed method of control, which was implemented in a laboratory drive system, is effective in reducing dc side current harmonics in a frequency range of 1300–3100 Hz, which is used by track circuits on railway lines, e.g., in Poland. The technique proposed by the authors allows taking into account any restrictions arising from the technical nature of low-frequency traction drives.**

***Index Terms*—DC–AC power conversion, electromagnetic compatibility (EMC), harmonics distortion, pulse-width modulation (PWM), rail transportation compatibility, selective harmonic mitigation (SHM), traction vehicles.**

I. Introduction

THE selective harmonic elimination (SHE) as a technique of inverter or rectifier modulation was described for the first time in the 1960s in [1] and disseminated by Patel and Hoft [2], [3]. Due to the limited technological capabilities of the power electronic of that time, the described method was considered to be difficult to implement and develop. The progress in technology of high-power semiconductor switches, digital signal processing, and control algorithms for hardware implementation is the reason why the SHE has recently gained new attention.

Currently, the SHE technique is applied in the industry as a method for improving the quality of electric energy that is converted by power electronic devices, such as inverters or controlled rectifiers. Generally, in the literature, as a criterion for assessing SHE technique's effectiveness, one assumes the coefficients of total harmonic distortion (THD) for voltage or current on an ac side of a converter [4], [5]. It stems from applying standards that define permissible values of a THD parameter and voltage harmonics content in an electric power system [6]–[8]. In [9] and [10], the examples of implementation of the SHE methods in both current and voltage source inverter (VSI) drive systems are proposed. Another application option was submitted in [11], where Zhao *et al.* developed the system based on the SHE modulation technique for active compensation of voltage harmonics in grid-connected inverters. However, the literature does not indicate examples of the application of the SHE method that has been proposed by the authors, i.e., for limiting dc-link and catenary current harmonics generated by traction drive systems equipped with VSIs. Moreover, the selective harmonic mitigation (SHM) technique [7] was taken under consideration by the authors to support the SHE technique and to increase the efficiency of the proposed method.

The issue of control and cancelation of dc-link current harmonics has been taken into consideration, as a traction compatibility problem, since first VSI traction drives started to operate on railways. One of the first solutions was based on reinjection into the dc-link for the detected current harmonics with opposite phase [12]. Nowadays, the idea of harmonics reinjection is considered to be risky due to the fact that the detuned reinjection system would provide additional harmonics of significant amplitude. The problem will escalate with the increment of harmonics frequency. The advantage of this solution was that the applicability was independent of a number of drives used on-board the vehicle. For multidrive vehicles (most of high and medium power traction vehicles), the cancelation methods were proposed [13], [14] as well as for stationary, grid-connected applications [15]. The current harmonics generated by parallel operating inverters are canceling each other. The efficiency of this method depends on the balance of drives

Manuscript received November 24, 2016; revised February 20, 2017; accepted March 13, 2017. Date of publication April 14, 2017; date of current version September 11, 2017. *(Corresponding author: Marcin Steczek.)*

M. Steczek is with the Institute of Electrical Power Engineering, Lodz University of Technology, 90-924 Lodz, Poland (e-mail: msteczek@p.lodz.pl).

P. Chudzik is with the Institute of Automatic Control, Lodz University of Technology, 90-924 Lodz, Poland (e-mail: pchudzik@p.lodz.pl).

A. Szeląg is with the Institute of Electrical Power Engineering, Warsaw University of Technology, 00-661 Warsaw, Poland (e-mail: adam.szelag@ee.pw.edu.pl).

Color versions of one or more of the figures in this paper are available online at http://ieeexplore.ieee.org.

Digital Object Identifier 10.1109/TIE.2017.2694357

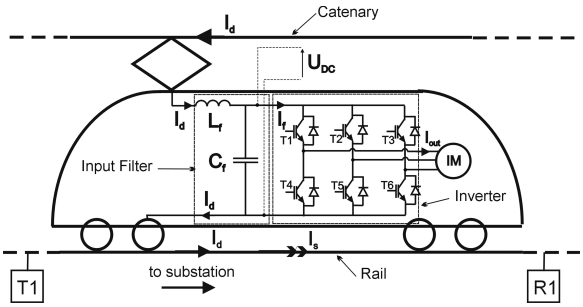

Fig. 1. Simplified scheme of the main circuit of a dc traction vehicle with a two-level voltage-source inverter (VSI).

loading conditions which is extremely difficult under traction conditions. The loading of the drives, on-board of a single vehicle, can differ due to the fact that the wheel diameter of an individual axle can be different. This leads to the situation that drives must operate with different frequencies and they are loaded unequally. Another disadvantage of this method is the fact that it is dependent on precise cooperation of two or more inverters. If one of them fails, method is ineffective. However, it might be effective in no-traction applications.

The method of dc-link current harmonics control that is proposed in the paper is free of disadvantages of mentioned methods. It is independent of loading balance between drives on-board the vehicle, because a switching strategy is determined for every drive separately and the even load between a vehicle's axle is not required. The described effect can be achieved by assuming that every individual drive on-board the vehicle is allowed to generate the current harmonics below limits divided by a number of drives used for propulsion of the vehicle (in the worst case, assuming simple summation of harmonics amplitudes). Results of simulation analysis and analytical calculations carried out by the authors were compared with the results of laboratory measurements. Additional advantage of the presented method is that synchronization of parallel inverters control is not required, which makes the method more reliable than other solutions described in the literature.

II. Compatibility Problem Description and Proposed Solution

The last two decades of rapid development of power electronics applications in electric traction rolling stock have led to numerous new solutions in main circuits of electric traction vehicles. In terms of a main circuit topology, currently the most popular solution is a vehicle driven by asynchronous motors supplied by two-level IGBT (VSI) [16], [17] (see Fig. 1).

Traction vehicles equipped with inverters are in fact significant source of electromagnetic interferences, both of conducted and radiated nature [18], [19]. The flow of the catenary current harmonics (I_d—Fig. 1) through the return circuit is able to disturb operation of track circuits (transmitter - T1, receiver - R1—Fig. 1) used to detect track occupancy in railway signaling, command, and control system, what constitutes a threat to railway traffic safety. That is the reason why the limits for I_d current harmonics are established by the operators of

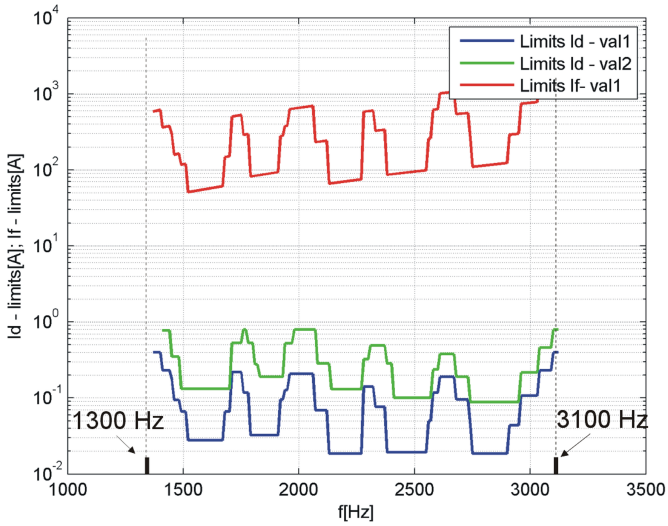

Fig. 2. Limits for catenary (I_d) and recalculated for dc-link (I_f) current harmonics, generated by a traction vehicle in the range of frequencies from 1300 to 3100 Hz; val1, val2—valid limits for Polish railway routes.

railway lines (e.g., PKP PLK S.A. in Poland—Fig. 2) in order to ensure correct operation of track circuits [20]. The frequency band that is the most exposed to the conducted distortions is the 1300-3100 Hz frequency span. The reason of this is the low level of signals used by track circuits operating with these frequencies and what follows, their high sensitivity to current harmonics. Two limit patterns for current I_d are specified (see Fig. 2): *val*1—limits valid for all railway routes in the whole country and *val*2—specified for railways routes, on which devices known to be more susceptible to current disturbances have been decommissioned. In this work, the more restrictive limits (*val*1) will be used as the evaluation criterion. Mentioned "I_d*-limits*" can be recalculated on the dc-link side of low-pass gamma-type input filter as the "*If-limits*."

Assuming that filter's impedance is linear for higher frequencies, the I_d current can be recalculated to I_f current, using impedances of the choke $Z_{\mathrm{Lf}}(j\omega)$ and the capacitor $Z_{\mathrm{Cf}}(j\omega)$ in the equation for an impedance current divider

$$I_f\,(j\omega) = I_d\,(j\omega) \cdot \left[\frac{Z_{\mathrm{Lf}}\,(j\omega)}{Z_{\mathrm{Cf}}\,(j\omega)} + 1\right]. \tag{1}$$

I_f*-limits* can be compared with I_f current harmonics whose magnitudes are much higher than I_d, what makes them easy to detect and measure (see Fig. 3).

In order to reduce I_d current harmonics to fulfill the required limits, the novel concept of applying the VSI modulation technique based on combination of a widely known SHE and SHM techniques is proposed for shaping a traction vehicle's catenary current (I_d) spectrum. The results of application the proposed technique were compared with standard sinusoidal pulse-width modulation (SPWM) modulations. Fig. 3 presents an example of comparison of VSI dc-link current spectra (limits recalculated on dc-link side—red solid lines) with the SPWM modulation and SHE/SHM method applied into the inverters simulation model with static *RL*-type load, for a set of inverter's operating points. When using the SPWM technique, the resulted dc-link

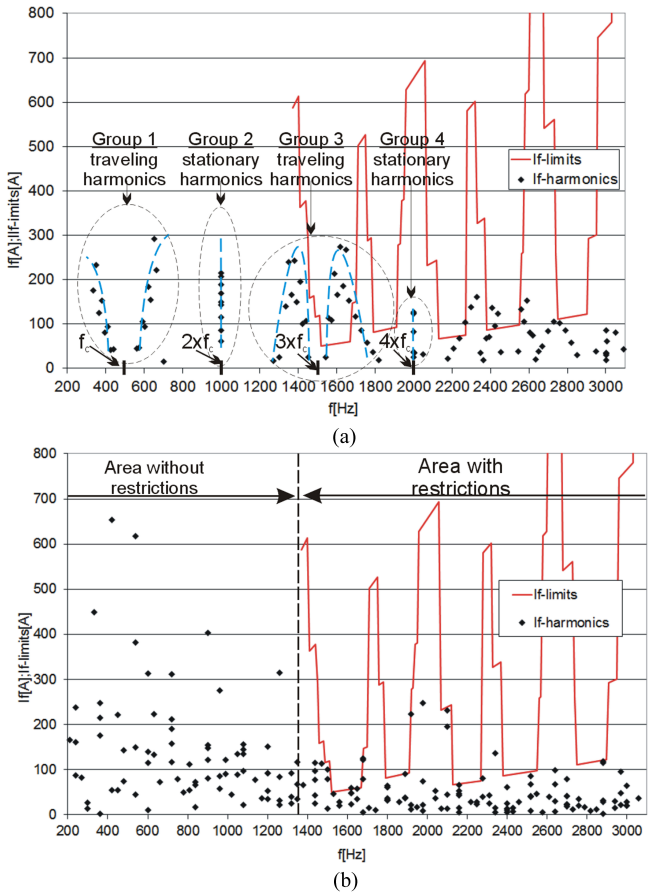

Fig. 3. Simulation of a dc-link I_f current harmonics spectrum of a traction drive system using static load model—"I_f-limits"—current harmonics limits recalculated on dc-link side of input filter: (a) SPWM modulation—one can observe exceeding of the assumed limits, and (b) proposed SHE/SHM method.

current harmonics can be divided into two groups: stationary and traveling. The frequency of stationary harmonics is given as

$$f_{\mathrm{If}\_s} = p \cdot f_c \text{ for even } p \tag{2}$$

where f_c is the carrier signal frequency.

Frequency of traveling harmonics is given as

$$f_{\mathrm{If}\_t} = p \cdot f_c \pm 3 \cdot f_{\mathrm{fal}} \text{ for odd } p \tag{3}$$

where f_{fal} is the basic output voltage component frequency.

The SHE or SHM are noncarrier techniques and due to this the frequency of inverter's output voltage V_{out} and current I_{out} harmonics depends only on f_{fal} and for a waveform with a half-wave symmetry is given by

$$f_{I\mathrm{out}\_h} = (3 \cdot p \pm 1) f_{\mathrm{fal}}, \quad p = 1, 2, 3, \ldots \tag{4}$$

and for a quarter wave symmetry is given by

$$f_{I\mathrm{out}\_q} = (6 \cdot p \pm 1) f_{\mathrm{fal}}, \quad p = 1, 2, 3, \ldots \tag{5}$$

The ac side inverter's output current I_{out} harmonics interlace into dc-link current I_f harmonics of frequency given for a half-wave symmetry by

$$f_{\mathrm{If}\_h} = (3 \cdot p) f_{\mathrm{fal}}, \qquad p = 1, 2, 3, \ldots \tag{6}$$

and for a quarter-wave symmetry given by

$$f_{\mathrm{If}\_q} = (6 \cdot p) f_{\mathrm{fal}}, \qquad p = 1, 2, 3, \ldots \tag{7}$$

When using SPWM modulation both stationary and traveling harmonics can overrun the assumed limits. Suitable SHE/SHM modulation sets all dc-link I_f current harmonics below the current harmonics limits calculated per dc-link side (see Fig. 3). This result constitutes a motivation for the authors to develop the proposed modulation method for a traction drive system model. It can be observed [see Fig. 3(b)] that when the SHE/SHM technique is applied, the amplification of low order I_f current harmonics can be expected. However, this effect occurs in the range of frequencies free from any restrictions. It has no influence on compatibility issue, which is the scope of this paper.

The analytical methods of the dc-link current harmonics calculation are reported in the literature [21], [22]. However, the mathematical determination of harmonics' values is beyond the scope of this paper aimed at presenting the novel concept of industrial application of SHE and SHM techniques in traction drives. The values of dc-link current harmonics can be precisely calculated using a simulation model described in Section IV-B and verified by means of laboratory measurements in Section IV-C.

The area of research was defined for a two-level VSI drive, because nowadays this solution is the most popular in main circuits of the latest traction vehicles. The authors are aware of research works conducted for three-level inverters for railway applications. However, application of presented modulation method in two-level inverters provides the solutions for already operating and produced in near future rolling stock.

Moreover, the use of three-level inverters on-board of railway traction vehicles is the solution not yet implemented as a standard solution and does not solve definitely described compatibility problem.

III. Theoretical Description of the SHE/SHM Technique

The paper presents the application of combination of SHE and SHM methods for solving the described problem. The following specific objectives were established:

1) shaping an inverter's output voltage waveform with an assumed basic component frequency and amplitude;
2) controlling the selected output voltage harmonics in such a manner so that the selected dc-link current harmonics do not reach the assumed limits; and
3) ensuring that an output voltage waveform is feasible by a voltage inverter with parameters corresponding to the parameters of a typical traction VSI.

The study concerns a half-bridge two-level VSI, which for many years has been the most widely used solution in main circuits of traction vehicles, which cooperate with a 3 kV dc electric traction power supply system. A generalized output voltage waveform of this type of an inverter has a shape as shown in Fig. 4 [1]–[3].

Applying the SHE or SHM technique, the three types of output waveform symmetry can be assumed: a quarter-wave

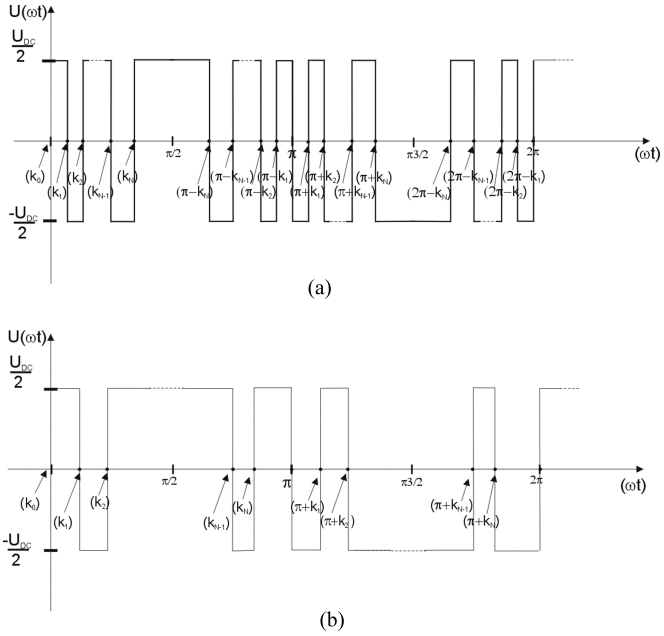

Fig. 4. Generalized voltage waveforms with—U_{dc}—supplying voltage: (a) Quarter-wave symmetry. (b) Half-wave symmetry.

symmetry or a half-wave symmetry or a nonsymmetrical. Depending on whether the assumed symmetry is obtained, various results should be expected depending on the number of eliminated harmonics, nature of a harmonics spectrum, harmonics phasing, performance of the inverter, and time of determining an optimal solution [23].

The function that describes this type of waveforms fulfills all Dirichlet's conditions, hence has a representation in a form of a Fourier's series and can be described by the following relation:

$$f(\omega t) = a_0 + \sum_{n=1}^{\infty} \left[a_n \sin(n\omega t) + b_n \cos(n\omega t)\right] \tag{8}$$

where a_0, a_n, and b_n are the coefficients described by Euler's formulas

$$a_0 = \frac{1}{2\pi}\int_0^{2\pi} f(\omega t)d(\omega t) \tag{9}$$

$$a_n = \frac{1}{\pi}\int_0^{2\pi} f(\omega t)\sin(n\omega t)d(\omega t) \tag{10}$$

$$b_n = \frac{1}{\pi}\int_0^{2\pi} f(\omega t)\cos(n\omega t)d(\omega t). \tag{11}$$

Assuming that the considered voltage waveform represents the half-wave symmetry, a function that describes the wave fulfills the following condition:

$$f(\omega t) = -f(\omega t + \pi). \tag{12}$$

Coefficients of a Fourier's series are described by the formulas

$$a_n = \begin{cases} \dfrac{2U_{\mathrm{dc}}}{n\pi}\left[1 + \sum_{i=1}^{M}(-1)^i \cos(n\cdot k_i)\right], & \text{for odd } n \\ 0, & \text{for even } n \end{cases} \tag{13}$$

$$b_n = \begin{cases} \dfrac{2U_{\mathrm{dc}}}{n\pi}\left[-\sum_{i=1}^{M}(-1)^i \sin(n\cdot k_i)\right], & \text{for odd } n \\ 0, & \text{for even } n \end{cases} \tag{14}$$

where U_{dc} is the dc-link voltage, M is the number of switching angles in a half-period, k_i is the ith switching angle of an inverter's transistor, and n is the harmonics order.

For a wave that is symmetrical in a quarter period, both conditions (12) (for half-wave symmetry) and (15) are fulfilled

$$f(\omega t) = f(\pi - \omega t). \tag{15}$$

For a waveform with quarter-wave symmetry, Fourier's series coefficients assume the following values:

$$a_n = \begin{cases} \dfrac{2U_{\mathrm{dc}}}{n\pi}\left[1 + 2\sum_{i=1}^{N}(-1)^i \cos(n\cdot k_i)\right], & \text{for odd } n \\ 0, & \text{for even } n \end{cases} \tag{16}$$

$$b_n = \begin{cases} 0, & \text{for odd } n \\ 0, & \text{for even } n \end{cases} \tag{17}$$

where N is the number of switching angles in a quarter period.

It follows from the above-mentioned considerations that in case of a wave symmetrical in relation to $\pi/2$, only the a_n coefficient for odd harmonics has a nonzero value (even harmonics are eliminated). In asymmetrical three-phase system, the triplen harmonics of phase voltage are cophasal and equal in magnitude. Thus, for a star-connected motor with an insulated neutral point, the phase voltages will cancel out between the line to line voltage and no line current of triplen harmonics will result. In this case, the a_n coefficient is a relative value of harmonics amplitudes of output phase voltage of $n = 5, 7, 11, 13\ldots$ order, expressed by the formula (5).

Upon determining whether the obtained voltage waveform fulfills the conditions of a quarter-wave symmetry (12), (15) and consists of an N number of switching angles in each quarter of a period, based on dependence (16), it is possible to create a system of N equations (18), as shown at the bottom of the next page.

Each of the above-mentioned equations is used to fix an amplitude for a selected voltage harmonic. This example shows a set of equations for N number of switching angles, which allows eliminating $N - 1$ voltage harmonics and determining an $M1$ value of a basic component, which is defined by the relation

$$M1 = \frac{2\cdot V_{\mathrm{ph}}}{U_{\mathrm{dc}}} \tag{19}$$

where V_{ph} is the eligible amplitude of an output voltage basic component and U_{dc} is the voltage supplying a drive system.

In formula (18), equations from 2nd to Nth have their right sides compared to zero, which is equivalent to application of the SHE method. If the right sides of a set of equations (18) are replaced by the vector of values of the selected harmonics (20), there is an opportunity of setting values of the selected

harmonics (SHM technique) described in [7] and [24]

$$\mathbf{M} = [M1; M2; M3; \ldots; MN]^T. \tag{20}$$

Using the method of harmonics mitigation gives a wide range of shaping opportunities for an inverter's output voltage harmonics, and consequently the dc-link current harmonics spectrum. The following conditions imposed on the calculated switching angles constitute an extremely important limitation of the proposed method:

First condition—calculated switching angles must be feasible by a traction inverter. At this stage, the most difficult part is to maintain the appropriate sequence of subsequent angles, which have to fulfill the following condition:

$$k_1 < k_2 < \cdots < k_{N-1} < k_N < \frac{\pi}{2}. \tag{21}$$

Second condition—switching frequency (SWF) for a single key cannot exceed its switching capacity, i.e., real transistors used in traction drive systems. This study adopts the permissible frequency of $f_t < 1200$ Hz that is given by the following formula:

$$f_{\mathrm{ti}} = \frac{2 \cdot \pi \cdot f_{\mathrm{fal}}}{(k_i - k_{i-1})}, \quad \text{for } i = 1, 2, \ldots, N+1. \tag{22}$$

where f_{fal} is the frequency of output voltage of basic component frequency and k_i is the ith inverter's switching angle.

Frequency f_t is established in the range of angles numbers $\langle 0; N+1 \rangle$. Due to the fact that the chosen waveform begins with a high state of transistor T1 [see Fig. 4(b)], there is an obligatory switch of the state at the beginning of each cycle in $k_0 = 0$. The k_{N+1} angle is the first one in the second quarter of the considered period [see Fig. 4(b)]: $k_{N+1} = (\pi - k_N)$. When the SHE/SHM equations and constraints are formulated, the solving tool must be chosen. There are a large number of studies on how to increase effectiveness of solving the formulated equations [4], [25]. The latest publication [26] presents implementation of Groebner's and the symmetric polynomials theory to solve SHE equations. The research on the improvement of the SHE problem solving method is still developing, increasing the calculations effectiveness [27]. There are also some studies on how to solve the SHE problem, based on application of optimization tools by means of formulating a cost function that includes the established assumptions (e.g., minimizing system power loss) [28] or the content of a harmonics group [29]. Literature also offers some insight on the opportunity of solving the SHE problem by means of genetic algorithms [30] as well as modern evolutionary algorithms, such as a bee algorithm [31] or a particle swarm optimization algorithm [32].

The increment of efficiency of solving method is out of the scope of this paper. Therefore, the authors decided to apply the MATLAB "fsolve" function, which uses the "trust-region-dogleg" algorithm to solve SHE and SHM equations.

IV. Verification of the SHE/SHM Method in an Inverter Drive System

After determining transistors switching angles k_i, it is necessary to determine the method for their implementation in inverter drives. The *offline* methods with storing the switching angles in *lookup table* or methods can be applied [33]. For the implementation of the *real-time* method, one should reduce time of calculations of the switching angles by avoiding the necessity of solving nonlinear transcendental equations. Proposed solution is to modify carrier-based modulation to the SHE technique [34]. At this stage of work, the *offline* method was chosen and calculated switching angles were stored in a *lookup table*. An important advantage of the presented offline method compared with the *real-time* methods is that the solution does not require increasing the processing power of the microcontroller and is suitable for implementation in the conventional inverter driver. Modulation strategy should be determined once for drives' whole operating live time. Therefore, to achieve objective established in this paper, there is no need to use costly microcontroller for real-time calculations.

The aim of the paper was to demonstrate that the SHE/SHM method can be used for shaping a dc-link current harmonics spectrum (and what follows—catenary current harmonics) in the inverter drive system, for the frequency range within the above-mentioned set limits [20]. For this purpose, one has developed a laboratory stand—a physical model of a traction drive system and a simulation model of a stand, which were used to determine efficiency of the proposed method. In order to verify the simulation model used for further research studies, the results of the conducted measurements were compared with the results of computer simulations.

A. Laboratory Stand

The typical topology of a 3 kV dc traction vehicle's main circuit consists of a low-pass *LC* input filter (with resonance frequency below 30 Hz) and a 6T topology VSI. In order to reflect the phenomena occurring in an actual traction drive, one

$$\begin{cases} \frac{4}{n_1\pi}[1 - 2\cos(n_1k_1) + 2\cos(n_1k_2) - \cdots \pm 2\cos(n_1k_N)] = M1 \\ \frac{4}{n_2\pi}[1 - 2\cos(n_2k_1) + 2\cos(n_2k_2) - \cdots \pm 2\cos(n_2k_N)] = 0 \\ \vdots \\ \frac{4}{n_N\pi}[1 - 2\cos(n_Nk_1) + 2\cos(n_Nk_2) - \cdots \pm 2\cos(n_Nk_N)] = 0 \end{cases} \tag{18}$$

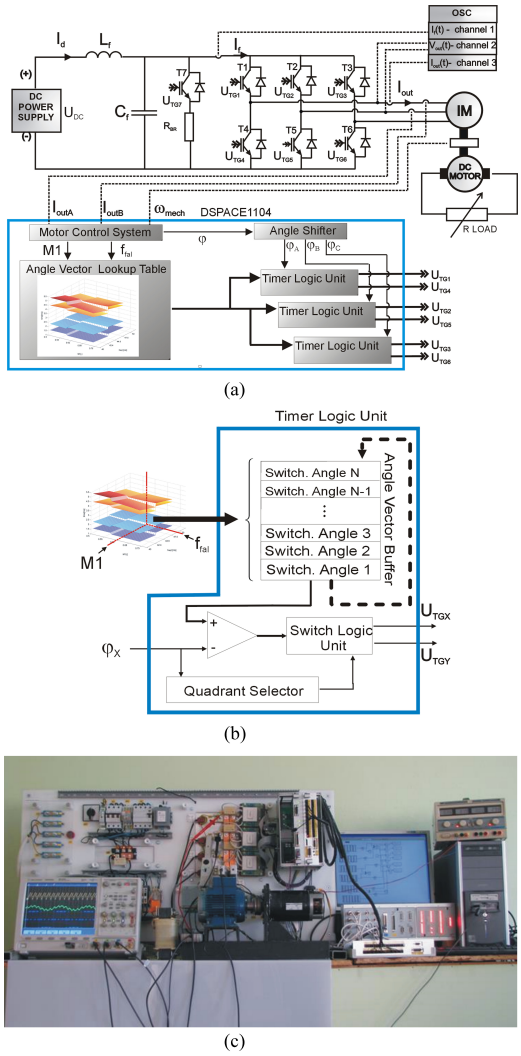

Fig. 5. Laboratory drive system: (a) simplified scheme, (b) scheme of timer logic unit, and (c) laboratory stand.

TABLE I
PARAMETERS OF A LABORATORY DRIVE SYSTEM

Symbol	Parameter	Value
	Type	Sf71-2B, Besel type
P	Rated power,	0.55 kW
$\cos\varphi$	Rated power factor	0.95
I_n	Rated current	1.37 A
n_o	Rated speed	2810 r/min
U_n	Rated voltage	$U_n = 380$ V
f_n	Rated frequency	$f_n = 50$ Hz
L_F	Input filter's inductance	4.7 mH
C_F	Input filter's capacitance	2.7 Mf

used a model of considerably low power (see Fig. 5). Table I summarizes basic parameters of this laboratory model.

At this stage of work, the DSPACE 1104 card and MATLAB SIMULINK software were used in a presented laboratory system. Due to the capabilities of the used equipment, it was possible to develop software model of modulator which implements the proposed modulation technique in laboratory drive.

Proposed technique allows for the implementation of the voltage modulator with ability of shaping the dc-link current

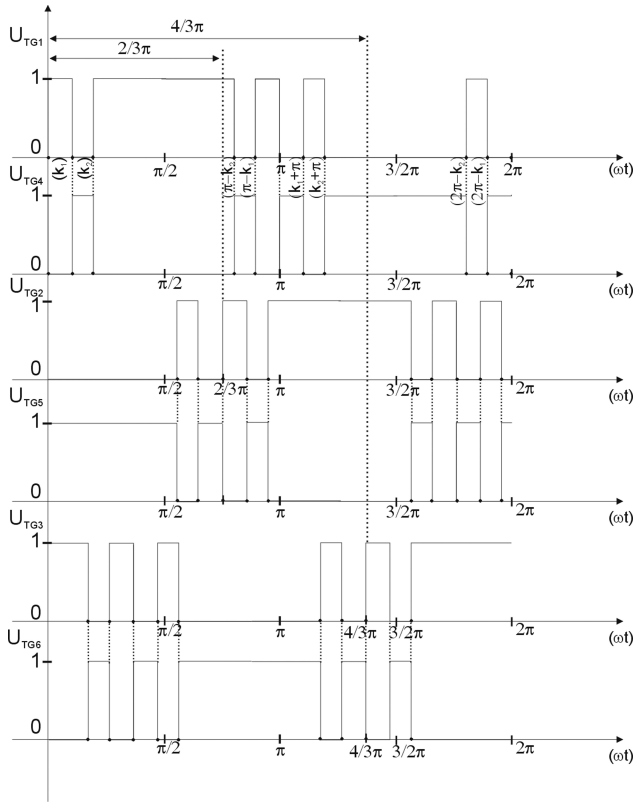

Fig. 6. Scheme of conversion of two switching angles (k_1, k_2) into control signals for six transistors in the three-phase VSI.

harmonic spectrum, without performing online calculations which is the novel approach for traction drives control. Input quantities for modulator are: relative value of fundamental voltage (M1), fundamental frequency (f_{fal}), and the angle of the voltage vector (φ). For particular M1 and f_{fal} provided by "motor control system," modulator draws the switching angles from the *lookup* table (*angle vector lookup table*), which was calculated *offline* by means of described in a paper SHE/SHM algorithm. Switching angles are stored in a buffer (*angle vector buffer*) and transformed into the system of three phase, VSI control waveforms U_{TG} (Fig. 6 presents the example for $N = 2$) by phase shifting provided by *"timer logic unit"* [see Fig. 5(b)] with respect to *"angle shifter"* (φ_A, φ_B, φ_C).

Assuming that the voltage module (M1) is given, in the lookup table, from 0 to 1.35 with 1% resolution and fundamental frequency (f_{fal}) is given from 0 to 60 Hz with 0.1 Hz resolution, two dimensions of the lookup table can be established—135 $\times$ 600. Making the exaggerated assumption that all operation points use 35 switching angles in quarter wave described by 24 bit number each, the size of stored lookup table can be calculated as 600 $\times$ 135 $\times$ 35 $\times$ 24 bit what gives 8 MB. This size will be never excided because with frequency increment the number of switching angels is being reduced and it is not obligatory that SHE/SHM should be implemented in whole range of drive operation.

The hardware implementation of the presented method in full-scale traction drive requires the use of small size of the programmable logic (FPGA or CPLD), to process *"angle vector*

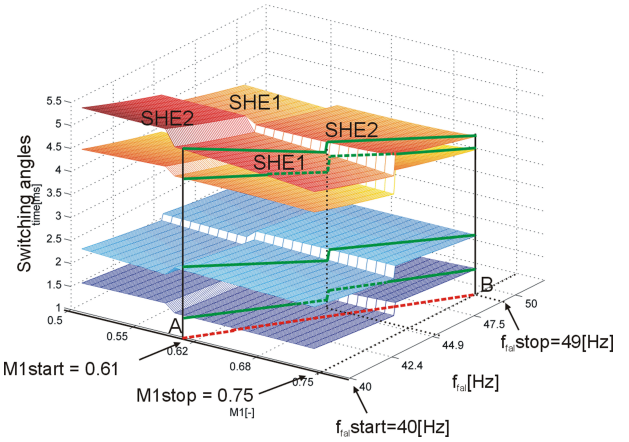

Fig. 7. Angle vector lookup table for SHE in operation range $M1 = 0.5$–0.75 and $f_{\mathrm{fal}} = 40$–49 Hz.

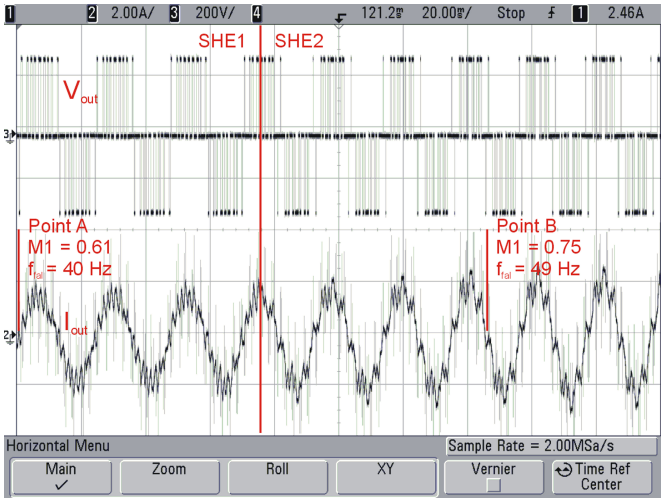

Fig. 8. Waveforms of inverter's output voltage V_{out} and current I_{out}.

buffer" without loading the microcontroller. For implementation of the proposed methods, it is sufficient to use the commonly used inverter's controllers such as: microcontrollers DSPiC32 or systems with processors ARM family with a programmable logic module. The only required enhancement is an 8 MB (maximum) RAM module. The work on the implementation of described modulator in FPGA family XILINX ZYNQ-7000 is in authors' work plan for the nearest future.

The correctness of described implementation was examined as well. The drive system was programmed to change the operating point from A to B (see Fig. 7) in time 140 ms with change of SHE modulation strategy in the meantime (SHE1-elimination of 5th, 7th, 11th V_{out} harmonic; SHE2-elimination of 5th, 7th, 13th V_{out} harmonic). Proposed implementation provides the possibility of fast change of frequency (f_{fal}), voltage value (M1), and modulation strategy smoothly presented in Fig. 8.

B. Simulation Model

At this stage of work, one used a model of an asynchronous motor fed by a voltage inverter, which is designed for calculation of quasi-steady-states (see Fig. 9). Fig. 9(b) presents scheme of

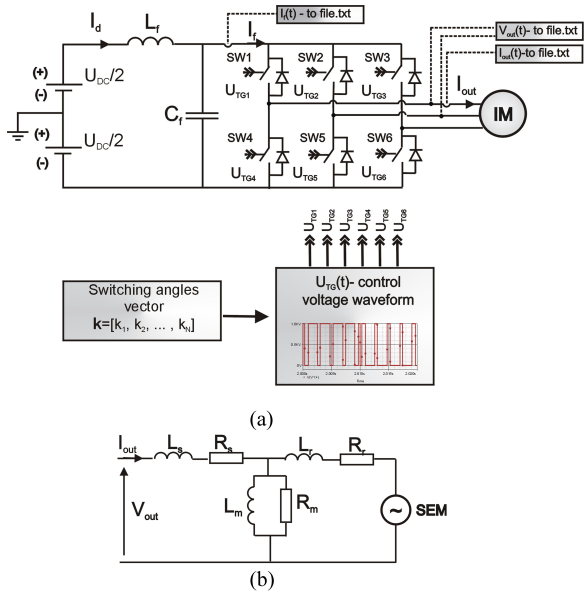

Fig. 9. Simulation model: (a) drive system scheme and (b) model of induction machine (one phase).

one phase in the induction machine model used in simulations where L_m is the magnetizing inductance; L_s is the per-phase stator leakage inductance; L_r is the per-phase rotor leakage inductance, R_s is the per phase stator winding resistance; R_r is the per phase rotor resistance, R_m is the core loss resistance; I_{out} is the per phase motor input current; V_{out} is the per phase motor input voltage; and SEM is the electromotive force.

In order to speed up the calculations, inverter transistors were replaced with switches, excluding snubber circuits. These simplifications do not affect the quality of the results in the examined range of relatively low-frequencies. Each examined operating point of a drive system was modeled as a separate steady state. The dc link current $I_f\,(t)$ waveforms were determined by means of simulation, and saved into a txt. Harmonics spectrum $(I_f(f))$ was determined by means of a fast Fourier transform (FFT) analysis with use of a Hanning window.

C. Measurement Verification of the Simulation Model

Measurement verification of a simulation model was conducted on the basis of the comparison of the results of measurements and simulation for five sets of switching angles marked as Z1; Z2; Z3; Z4; Z5. Sets of switching angles were calculated for the following frequency of inverter's voltage basic component $f_{\mathrm{fal}} = 10; 20; 30; 40; 50$ Hz. Parameters of sets of switching angles are presented in Table II. Sets of switching angles were selected as examples used to demonstrate the accuracy of the used simulation model in modeling the dc-link I_f current spectrum of VSI with SHE and SHM modulations implemented.

Fig. 10 presents comparison of the measured and simulated currents and voltage waveforms in the described drive system. Fig. 11 presents an example of a comparison of dc-link current harmonics spectrum (I_f) measured in the laboratory drive system and calculated using the computer simulation with the described model. The paper focuses on the opportunity of

TABLE II
DATA OF THE SELECTED SETS OF THE SWITCHING ANGLES

Number of a set	f_{fal} [Hz]	N	$M1$ [–]	M_x [–]	k_x [rad]
Z1	10	8	0.3	$M_5 = M_7 = M_{11} =; = M_{13} = M_{17} = = M_{23} = 0.02; M_{19} = 0.04;$	$k_1 = 0.0478\ k_2 = 0.2080\ k_3 = 0.4430\ k_4 = 0.5996\ k_5 = 0.8541\ k_6 = 1.0187\ k_7 = 1.2929\ k_8 = 1.4476$
Z2	20	4	0.3	$M_5 = 0.1; M_7 = M_{11} = 0;$	$k_1 = 0.1066\ k_2 = 0.5189\ k_3 = 0.6292\ k_4 = 0.9859$
Z3	30	4	0.5	$M_5 = 0.1; M_7 = M_{11} = 0;$	$k_1 = 0.1548\ k_2 = 0.4572\ k_3 = 0.6649\ k_4 = 0.9593$
Z4	40	2	0.7	$M_5 = 0.1$	$k_1 = 0.3894\ k_2 = 0.7954$
Z5	50	2	0.9	$M_5 = 0.1$	$k_1 = 0.4447\ k_2 = 0.7134$

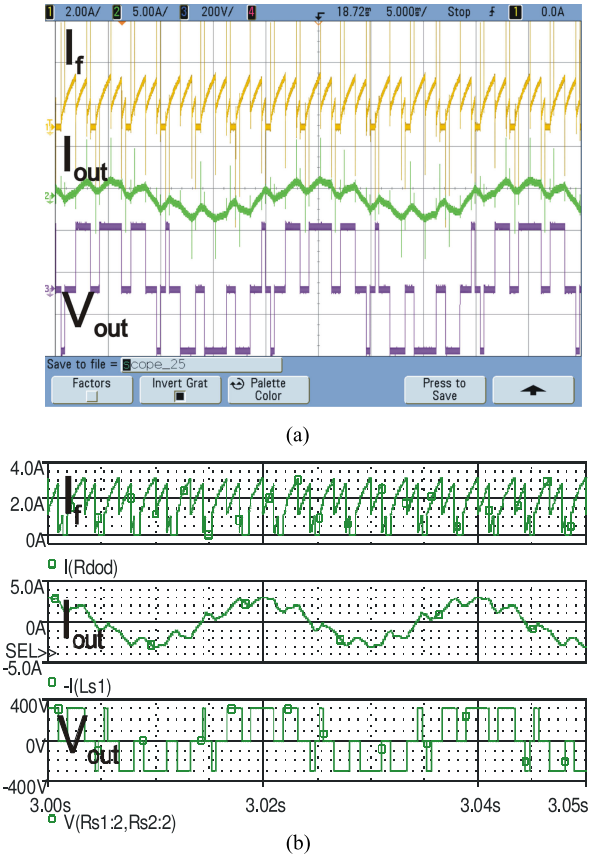

Fig. 10. Waveforms of dc-link current (I_f), inverter's output current (I_{out}), inverter's output voltage (V_{out}): (a) measurements and (b) simulation.

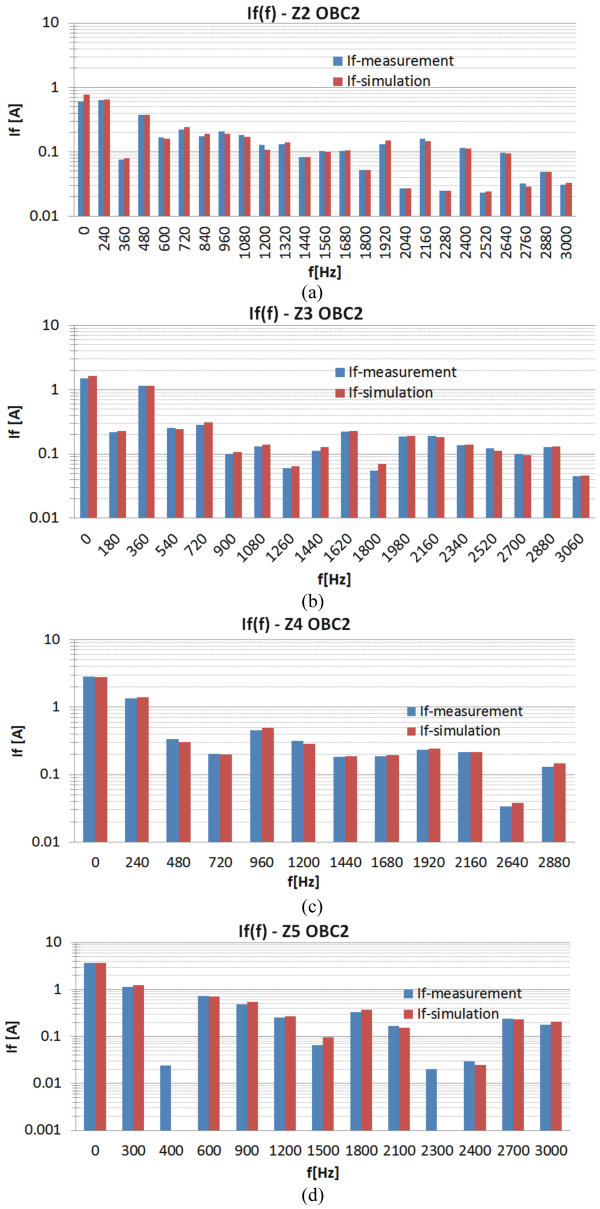

Fig. 11. Comparison of the measurements and simulation results for sets: (a) Z2; (b) Z3; (c) Z4; and (d) Z5.

applying the combination of SHE and SHM methods for I_f current spectrum shaping, and because of that the current spectrum will be a criterion for verifying the proposed simulation model. The difference between results of the simulation and measurements, in the range of frequencies 1300–3100 Hz, did not exceed $\Delta I_f = 30$ mA.

When analyzing the spectrum for Z5 [see Fig. 11(b)], it may be observed that some harmonics 400 and 2300 Hz occur in the measurements and are absent in the simulations. That can be described as the result of motor's rotor shape influence for rated frequency $f_{\mathrm{fal}} = 50$ Hz. The additional measured current harmonics are negligible, below assumed difference level $\Delta I_f = 30$ mA. Thus, this phenomenon was not included into the simulation model. Therefore, it may be concluded that the configured simulation model is accurate enough to be used at further stages of the study.

V. TUNING A DC-LINK CURRENT HARMONICS SPECTRUM TO THE LIMITS

A. SHE/SHM Method Algorithm

The algorithm of tuning the I_f current harmonics spectrum to the set limits is proposed. Each tested operating point of a drive system is defined as a frequency of inverter's output voltage basic component f_{fal} [Hz] and its relative value $M1$ [–] in regard to half of a supply voltage $U_{\mathrm{dc}}/2$. The aim of the

algorithm, described in this section, is to select harmonics that are eliminated and mitigated in a V_{out} voltage spectrum, in such a manner so the current spectrum I_f fulfills the set limits ($I_{\text{lim}}\,(I_f(f) < I_{\text{lim}}(f))$.

The tuning algorithm is formulated as the trial-and-error procedure based on the FFT analysis of the I_f spectrum, after each tuning step. The optimization algorithms can be as well used when additional constraints will be taken under consideration (such as: amplitude and value of uncontrolled harmonics, voltage THD on the inverter's ac side, simultaneous torque harmonics minimization [35], etc.).

The applied algorithm, for one operating point, can be described in a step-by-step scheme as follows:

1) Selection of the inverter's operating point—f_{fal}, $M1$,
2) Selection of a number of switching angles regarding the maximum inverter's SWF—N,
3) *Iteration* 1—Implementation of the SHE technique. Select the $N-1$ number of V_{out} harmonics, of the lowest possible order, for elimination —$M5 = M7 = M11, \ldots = 0$,
4) Analyze the I_f current spectrum, using the simulation model, and match with assumed limits. When no limits overruns detected ($I_f(f) < I_{\text{lim}}(f)$): end the procedure,
5) If the limits overruns are detected implement the SHM technique: *Iteration* 2—increase the V_{out} eliminated harmonic of the highest order by adding the assumed *dMx* value—$Mx = Mx + dMx$,
6) Analyze the I_f current spectrum, using simulation model, and match with the assumed limits. When there are no limits overruns ($I_f(f) < I_{\text{lim}}(f)$): end the procedure,
7) If the limits overruns are still detected run points 5) and 6) with increasing the iteration number (Iteration 2, Iteration 3, ...) until $I_f(f) < I_{\text{lim}}(f)$ or *Mx* exceeds its assumed maximum value *Mxmax*. When $Mx = Mxmax$ then change the mitigated harmonics order, and
8) Repeat steps 5–7 until: $I_f(f) < I_{\text{lim}}(f)$.

The above-described algorithm must be repeated for every operation point taken under consideration. All calculations are conducted *offline* and calculated switching angles are stored in a *lookup-table* as a switching pattern ready for implementation in the real drive system. Fig. 12 presents the example of influence of 11th ($M11 = 0$–0.19) V_{out} harmonic mitigation on the other voltage [see Fig. 12(b)] and dc-link I_f current [see Fig. 12(b)] harmonics with no assumed limits.

B. Implementation of the SHE/SHM Method in an Inverter Drive System

Described in Section V-A, algorithm was processed *offline* for all chosen operating points (see Table IV) of the laboratory drive. Using the described method, the switching angles were determined *offline* for the assumed operating range of the inverter. *N*-dimensional array was established, including sets of angles for modulation $M1 \in \langle 0.35,\ 1.4\rangle$ and basic component frequency $f_{\text{fal}} \in \langle 20,\ 60\rangle$. The derived array allowed for the implementation of an algorithm to the real-time control of the voltage and frequency of the inverter.

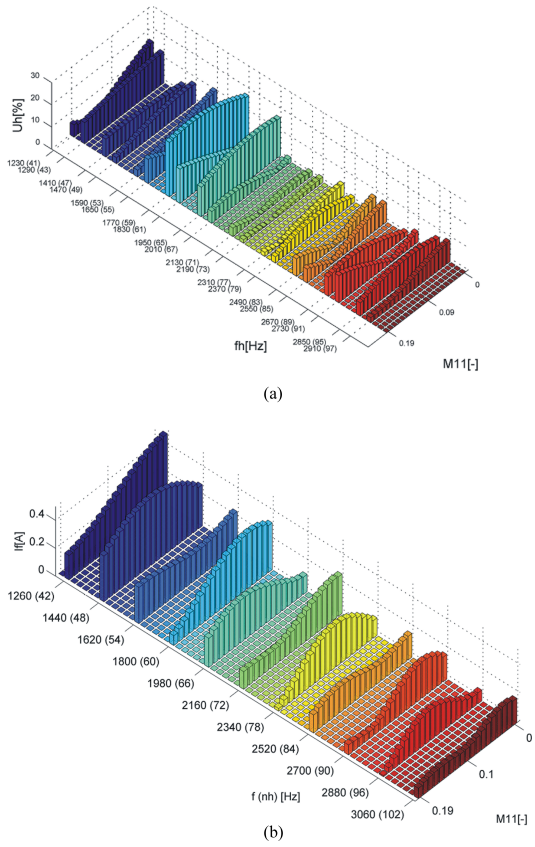

Fig. 12. Harmonic spectrum of the voltage-source inverter as a function of *M*11 harmonic change in the range of 0–0.19 ($M1$ = const. = 0.5; $f_{\text{fal}} = 30$ Hz)—simulation results; nh—harmonic order: (a) output voltage V_{out} and (b) dc-link current I_f.

Fig. 13 shows the example of the tuning process only for one operating point ($M1 = 0.5$; $f_{\text{fal}} = 30$ Hz). The results were obtained from both, simulations [see Fig. 13(b)] and measurements [see Fig. 13(b)]. The proposed tuning process in this case required five iterations. As it was mentioned before, the *iteration I* implements the SHE technique for selected V_{out} harmonics (5th,7th, and 11th—set Z31).

Due to the fact that 1620 Hz I_f current harmonic exceeds the forbidden level, *iteration II* provides the SHM technique for voltage harmonic of the highest order from eliminated ones—in this case 11th. (set Z34—$Mx = M11 = 0.05$). At this stage, the set of SHM equations can be described as follows:

$$\begin{cases} \dfrac{4}{\pi}[1-2\cos(k_1)+2\cos(k_2)-2\cos(k_3)] = 0.5 \\ \dfrac{4}{5\cdot\pi}[1-2\cos(5\cdot k_1)+2\cos(5\cdot k_2)-2\cos(5\cdot k_3)] = 0 \\ \dfrac{4}{7\cdot\pi}[1-2\cos(7\cdot k_1)+2\cos(7\cdot k_2)-2\cos(7\cdot k_3)] = 0 \\ \dfrac{4}{11\cdot\pi}[1-2\cos(11\cdot k_1)+2\cos(11\cdot k_2) \\ \qquad -2\cos(11\cdot k_3)] = Mx \end{cases} \tag{23}$$

where $M_x \in \langle 0,\ M_{x\max}\rangle$.

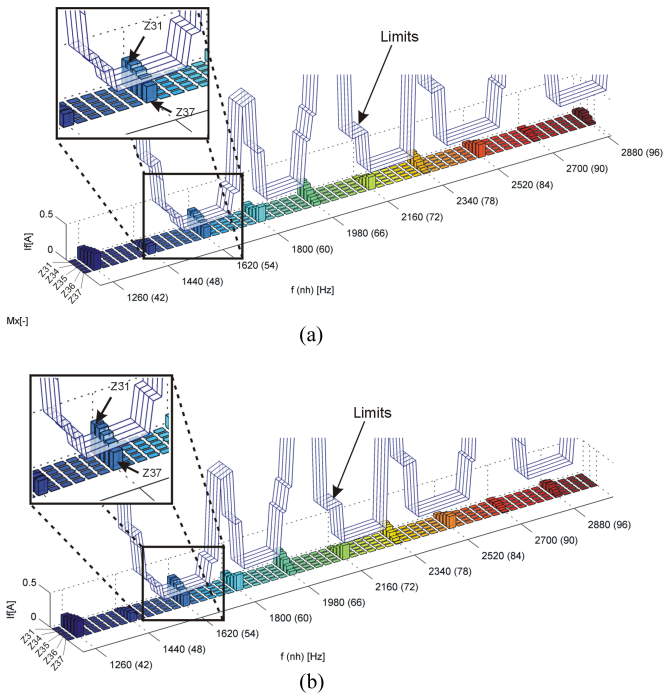

Fig. 13. DC-link current (I_f) harmonics and limits during spectrum tuning process: (a) simulation results and (b) measurements results.

TABLE III
PARAMETERS OF TUNING STEPS

Iteration No.	Set	N	$M1$ [–]	M_x [–]	k_x [rad]
Iteration I (SHE)	Z31	4	0.5	$M_5 = M_7 = 0$; $\boldsymbol{M}_{11} = 0$	$k_1 = 0.1451$; $k_2 = 0.4819$; $k_3 = 0.6655$; $k_4 = 0.9443$
Iteration II (SHM)	Z34	4	0.5	$M_5 = M_7 = 0$; $\boldsymbol{M}_{11} = 0.05$	$k_1 = 0.1513$; $k_2 = 0.4892$; $k_3 = 0.6721$; $k_4 = 0.9463$
Iteration III (SHM)	Z35	4	0.5	$M_5 = M_7 = 0$; $\boldsymbol{M}_{11} = 0.10$	$k_1 = 0.1573$; $k_2 = 0.4967$; $k_3 = 0.6790$; $k_4 = 0.9483$;
Iteration IV (SHM)	Z36	4	0.5	$M_5 = M_7 = 0$; $\boldsymbol{M}_{11} = 0.15$	$k_1 = 0.1631$; $k_2 = 0.5042$; $k_3 = 0.6862$; $k_4 = 0.9506$;
Iteration V (SHM)	Z37	4	0.5	$M_5 = M_7 = 0$; $\boldsymbol{M}_{11} = 0.19$	$k_1 = 0.1677$; $k_2 = 0.5103$; $k_3 = 0.6921$; $k_4 = 0.9525$;

Characteristic parameters for all steps are presented in Table III. Increment of 11th V_{out} voltage harmonic value to $Mx = M_{11} = 0.19$ (set Z37) delivers a positive result that means all I_f harmonics are below the assumed limits. Other operating points, mentioned in Table IV, were analyzed with the similar approach giving positive results in whole range of inverter's operating frequencies $f_{\text{fal}} = 20$–60 Hz [see Fig. 15(b)].

C. Comparison With SPWM Modulation Techniques

To confirm the efficiency of the proposed method, further laboratory examinations were carried out. In this section, the spectrum of measured I_f current, using the proposed SHE/SHM technique [see Fig. 15(b)], was compared with I_f current generated using the standard SPWM techniques [see Fig. 15(b) and (b)]. Only harmonics with amplitudes above 0.02 A are placed at graphs. Fig. 15 presents measurement results for six operating

TABLE IV
PARAMETERS OF MEASURED OPERATING POINTS

Point No.	f_{fal} [Hz]	$M1$ [–]	N (SHE-SHM)	Fc [Hz]	fc1 [Hz]	fc2 [Hz]
1	20	0.35	17	800	720	–
2	30	0.5	11	800	720	–
3	40	0.7	8	800	720	–
4	50	0.9	7	800	–	900
5	50	1.0	7	800	–	900
6	60	1.15/1.4*	3	800	–	900

*In overmodulation area for SHE/SHM $M1 = 1.15$ for SPWM $M1 = 1.4$.

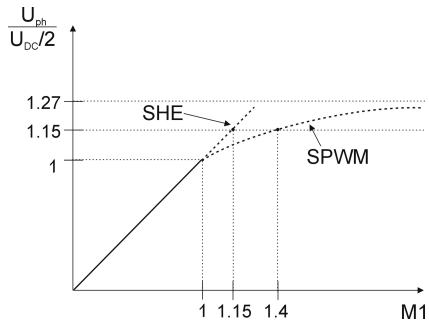

Fig. 14. Modulation index $M1$ for SHE/SHM and SPWM techniques versus voltage per motor phase. U_{ph}—amplitude of motor phase voltage.

points each (see Table IV) gathered in a single plot. Two SPWM techniques were used: synchronized SPWM with one of two carrier frequencies ($f_{c1} = 720$ Hz or $f_{c2} = 900$ Hz) and unsynchronized SPWM with constant carrier frequency $f_c = 800$ Hz. It means that the frequencies of stationary harmonics for synchronized SPWM depend on two frequencies (f_{c1} or f_{c2}). In both cases, the moving and stationary groups of I_f current harmonics can be identified, which coincides with the theoretical considerations presented in Section II [see Fig. 3(b)]. For both SPWM modulations, the limits overruns are detected for traveling and stationary harmonics. The area of operation for $M1 > 1$ was taken under consideration as well (point no. 6). For the SHE/SHM technique, the relationship between M1 and motor phase voltages is linear. For SPWM techniques, this area of overmodulation is nonlinear (see Fig. 14). Regarding equal phase voltages for considered modulations, $M1 = 1.15$ for SHE/SHM corresponds to $M1 = 1.4$ for SPWM. In the overmodulation area, the effective SWF in SPWM is decreasing due to the fact that switching points are dropped. To make results comparable, regarding the SWF, the number of switching angles for the SHE/SHM technique in point no. 6 was reduced.

The influence of the proposed method on THDI of motor phase current and switching losses is presented in Table V. Switching losses are proportional to SWF. For all analyzed operation points, the SWF for SHE/SHM was set below the ones used in SPWM techniques. Moreover, increment of THDI is not significant (maximum 2%). Taking into account that minimization of THDI is out of the scope of this paper, and it is less important, from the point of view of this study, than fulfilling compatibility restrictions, this result is recognized as satisfactory.

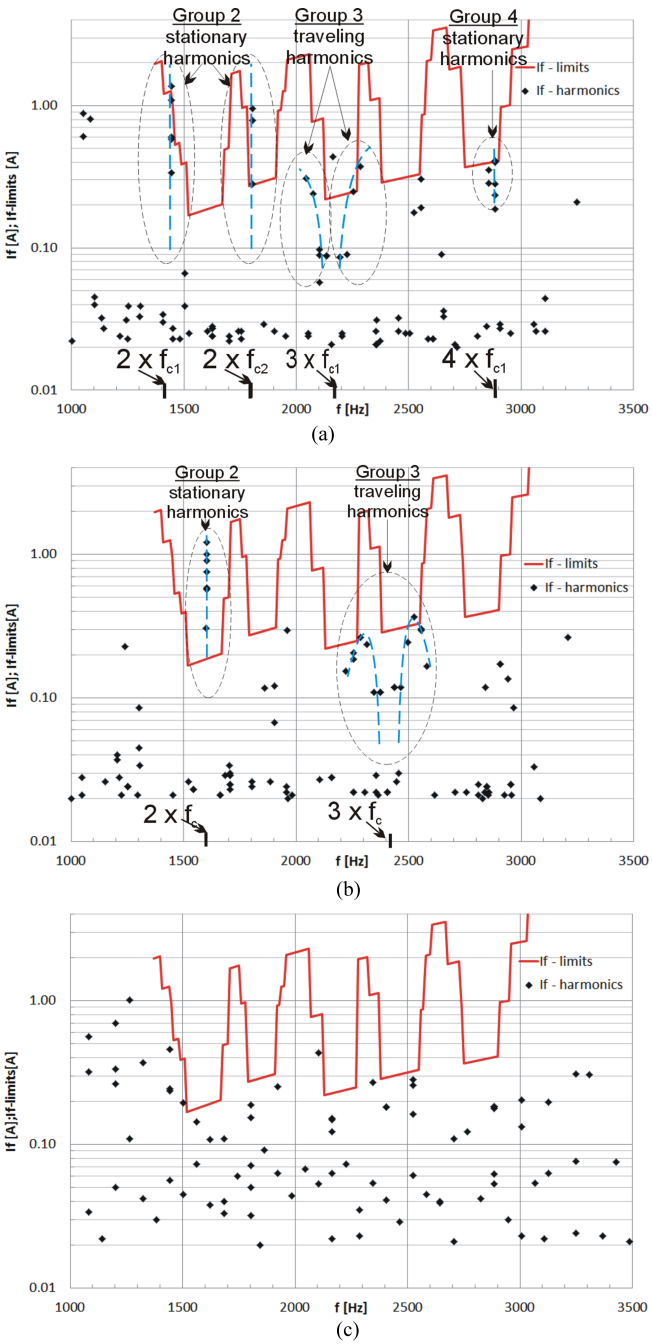

Fig. 15. Measured dc-link current (I_f) harmonics and limits for chosen modulation techniques: (a) synchronized SPWM, (b) unsynchronized SPWM, and (c) proposed SHE/SHM method.

TABLE V
RESULTS FOR MEASURED OPERATING POINTS

	SWF [Hz]	SWF [Hz]	SWF [Hz]	THDI [%]	THDI [%]	THDI [%]
Point No.	SHE/SHM	SPWM fc	SPWM fc1/fc2	SHE/SHM	SPWM fc	SPWM fc1/fc2
1	700	800	720	8.1	7.7	8.4
2	690	800	720	9.3	9.7	9.0
3	680	800	720	10.4	8.4	9.0
4	750	800	900	7.7	8.1	7.7
5	750	800	900	6.9	8.6	7.8
6	420	450	420	8.8	7.1	8.5

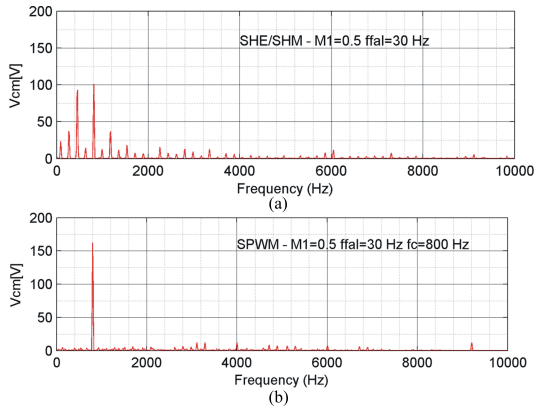

Fig. 16. Spectra of common mode voltage $V_{\rm cm}$ for point no. 2. (a) Proposed SHE/SHM modulation and (b) SPWM modulation.

The proposed SHE/SHM method provides positive results for every considered operating point that means no I_f current harmonics overrun the assumed limits what is proven by measurements [see Fig. 15(b)].

The influence of proposed modulation technique on common mode voltage ($V_{\rm cm}$) was investigated (see Fig. 16). For the SHE/SHM technique, $V_{\rm cm}$ spectrum is more distracted. It consists of higher number of harmonics of lower value than for the SPWM modulation technique. No overvoltage was observed, that means the proposed modulation is not affecting the motor bearings and insulation more than the standard SPWM.

VI. CONCLUSION

A new method of shaping the dc-link current spectrum in VSI traction drives was presented in this paper. The method was based on combination of SHE and SHM PWM techniques. It was shown that through a proper selection of eliminated/mitigated inverter's output voltage harmonics, one can shape a dc-link current spectrum to meet the limits imposed on catenary current harmonics. The limits were provided by railway operators to assure the compatibility between devices of railway control and signaling system and rolling stock. Presented technique of shaping the current harmonics spectra was a novel approach to traction VSI modulation strategy and it was fully feasible for implementation in modern full-scale traction drives.

The results of computer simulation were verified by means of laboratory measurements for a low-power drive. To prove the efficiency of the analyzed method, the proposed SHE/SHM technique was compared with synchronized and unsynchronized SPWM techniques (see Fig. 15). The application of the proposed algorithm allowed for deriving the inverters' switching strategy, which provided the dc-link current spectrum below the assumed limits for all analyzed operating points.

The presented method of shaping the dc-link current spectrum was independent of the traction motors' load unbalance and synchronization of inverters, what made it more reliable than known methods of harmonics cancelation and control. Moreover, this method was flexible enough to determine the switching strategy of VSI drives used in traction vehicles of different topologies with multiple limits for catenary current harmonics.

REFERENCES

[1] F. G. Turnbull, "Selected harmonic reduction in static dc-ac inverters," *IEEE Trans. Commun. Electr.*, vol. 83, no. 73, pp. 374–378, Jul. 1964, doi: 10.1109/TCOME.1964.6541241.

[2] H. S. Patel and R. G. Hoft, "Generalized techniques of harmonic elimination and voltage control in thyristor inverters: Part I–Harmonic elimination," *IEEE Trans. Ind. Appl.*, vol. IA-9, no. 3, pp. 310–317, May 1973, doi: 10.1109/TIA.1973.349908.

[3] H. S. Patel and R. G. Hoft, "Generalized techniques of harmonic elimination and voltage control in thyristor inverters: Part II–voltage control techniques," *IEEE Trans. Ind. Appl.*, vol. IA-10, no. 5, pp. 666–673, Sep. 1974, doi: 10.1109/TIA.1974.349239.

[4] J. N. Chiasson, L. M. Tolbert, and K. J. McKenzie, "A complete solution to the harmonic elimination problem," *IEEE Trans. Power Electron.*, vol. 19, no. 2, pp. 491–499, Mar. 2004, doi: 10.1109/TPEL.2003.823207.

[5] V. Mohan, S. Jeevananthan, and J. Raja, "An on-line adaptive filtering for selective elimination of dominant harmonics from line currents of a VSI fed drive using recursive least square algorithm," in *Proc. IEEE Int. Conf. Adv. Eng., Sci. Manage.*, 2012, pp. 773–778.

[6] *Voltage Characteristics of Electricity Supplied by Public Distribution Systems*, Std. PN-EN 50160, 2008.

[7] J. Napoles, J. I. Leon, R. Portillo, L. G. Franquelo, and M. A. Aguirr, "Selective harmonic mitigation technique for high-power converters," *IEEE Trans. Ind. Electron.*, vol. 57, no. 7, pp. 2315–2323, Jul. 2010, doi: 10.1109/TIE.2009.2026759.

[8] M. Sharifzadeh *et al.*, "Hybrid SHM-SHE pulse amplitude modulation for high power four-leg inverter," *IEEE Trans. Ind. Electron.*, vol. 63, no. 11, pp. 7234–7242, Nov. 2016, doi: 10.1109/TIE.2016.2538204.

[9] Y. Zhang and Y. Li, "Investigation and suppression of harmonics interaction in high-power PWM current-source motor drives," *IEEE Trans. Power Electron.*, vol. 31, no. 2, pp. 668–679, Feb. 2015, doi: 10.1109/TPEL.2014.2310955.

[10] A. Sanchez-Ruiz, G. Abad, S. Alvarez, and L. M. Tolbert, "Modulation selection procedure applied to a high-power adjustable high-speed drive," in *Proc. Eur. Conf. Electron. Appl.*, 2013, pp. 1–10, doi: 10.1109/EPE.2013.6631918.

[11] H. Zhao, T. Jin, S. Wang, and L. Sun, "A real-time selective harmonic elimination based on a transient-free inner closed-loop control for cascaded multilevel inverters," *IEEE Trans. Power Electron.*, vol. 31, no. 2, pp. 1000–1014, Feb. 2016, doi: 10.1109/TPEL.2015.2413898.

[12] C. Broche, J. Lobry, P. Colignon, and A. Labart, "Harmonic reduction in dc link current of a PWM induction motor drive by active filtering," *IEEE Trans. Power Electron.*, vol. 7, no. 4, pp. 633–643, Oct. 1992, doi: 10.1109/63.163643.

[13] H. Ye and A. Emadi, "An interleaving scheme to reduce dc-link current harmonics of dual traction inverters in hybrid electric vehicles," in *Proc. IEEE Appl. Power Electron. Conf. Expo.*, 2014, pp. 3205–3211, doi: 10.1109/APEC.2014.6803764.

[14] T. Ogawa and S. Wako, "Theoretical analysis of cancellation of dc-link current harmonics in the inverter-controlled dc electric railcar," in *Proc. IEEE Eur. Conf. Power Electron. Appl.*, Sep. 2007, pp. 1–10.

[15] Y. Yang, P. Davari, F. Zare, and F. BlaabJerg, "A dc-link modulation scheme with phase-shifted current control for harmonic cancellations in multidrive applications," *IEEE Trans. Power Electron.*, vol. 31, no. 3, pp. 1837–1840, Mar. 2016, doi: 10.1109/EPE.2007.4417469.

[16] J. Hu, W. Liu, and J. Yang, "Application of power electronic devices in rail transportation traction system," in *Proc. 37th IEEE Int. Symp. Power Semicond. Devices*, 2015, pp. 7–12, doi: 10.1109/ISPSD.2015.7123376.

[17] A. Marzouki, M. Hamouda, and F. Fnaiech, "A review of PWM voltage source converters based industrial applications," in *Proc. Int. Conf. Elect. Syst. Aircr., Railway, Ship Propulsion Road Veh.*, 2015, pp. 1–6, doi: 10.1109/ESARS.2015.7101520.

[18] A. Ogusola and A. Mariscotti, *Electromagnetic Compatibility in Railways - Analysis and Management*. Heidelberg, Germany: Springer, 2012, pp. 59–91.

[19] A. Szelag and M. Patoka, "Issues of low frequency electromagnetic disturbances measurements in traction vehicles equipped with power electronics drive systems," *Przegląd Elektrotech.*, vol. 9, pp. 290–296, 2013.

[20] A. Białoń *et al.*, "Defining limits and levels of disturbances in signalling and control railway systems," Railway Institute, Warsaw, Poland, Rep. 4430/10 for PKP PLK S.A., Sep. 2011 (in Polish).

[21] M. H. Bierhoff and F. W. Fuchs, "DC-link harmonics of three-phase voltage-source converters influenced by the pulsewidth-modulation strategy—An analysis," *IEEE Trans. Ind. Electron.*, vol. 55, no. 5, pp. 2085–2092, May 2008, doi: 10.1109/TIE.2008.921203.

[22] B. P. McGrath and D.G. Homes, "A general analytical method for calculating inverter dc-link current harmonics," *IEEE Trans. Ind. Appl.*, vol. 45, no. 5, pp. 1851–1859, Sep./Oct. 2009, doi: 10.1109/TIA.2009.2027556.

[23] M. S. A. Dahidah, G. Konstantinou, N. Flourentzou, and V. G. Agelidis, "On comparing the symmetrical and non-symmetrical selective harmonic elimination pulse-width modulation technique for two-level three-phase voltage source converters," *IET Power Electron.*, vol. 3, no. 6, pp. 829–842, 2010, doi: 10.1049/iet-pel.2009.0306.

[24] J. L. Leon, S. Kouro, L. G. Franquelo, J. Rodrigez, and B. Wu, "The essential role and the continuous evolution of modulation techniques for voltage-source inverters in the past, present, and future power electronics," *IEEE Trans. Ind. Electron.*, vol. 63, no. 5, pp. 2688–2701, May 2016, doi: 10.1109/TIE.2016.2519321.

[25] F. Swift and A. Kamberis, "A new walsh domain technique of harmonic elimination and voltage control in pulse-width modulated inverters," *IEEE Trans. Power Electron.*, vol. 8, no. 2, pp. 170–185, Mar. 1993, doi: 10.1109/63.223969.

[26] K. Yang, Q. Zhang, R. Yuan, W. Yu, J. Yuan, and J. Wang, "Selective harmonic elimination with Groebner bases and symmetric polynomials," *IEEE Trans. Power Electron.*, vol. 31, no. 4, pp. 2742–2752, Apr. 2016.

[27] K. Yang, L. Chen, J. Zhang, J. Hao, and W. Yu, "Parallel resultant elimination algorithm to solve the selective harmonics elimination problem," *IET Power Electron.*, vol. 9, no. 1, pp. 71–88, 2016, doi: 10.1109/TPEL.2015.2447555.

[28] J. R. Wells, B. M. Nee, P. L. Chapman, and P. T. Krein, "Optimal harmonic elimination control," in *Proc. 35th Annu. IEEE Power Electron. Spec. Conf.*, Aachen, Germany, 2004, pp. 4214–4219, doi: 10.1109/PESC.2004.1354745.

[29] M. Lewandowski and A. Szelag, "Minimizing harmonics of the output voltage of the chopper inverter, electrical engineering," *Arch. fur Elektrotech.*, vol. 69, pp. 223–226, 1986.

[30] E. Deniz, O. Aydogmus, and Z. Aydogmus, "GA - Based optimization and ANN-based SHEPWM generation for two-level inverter," in *Proc. IEEE Int. Conf. Ind. Technol.*, 2015, pp. 738–744, doi: 10.1109/ICIT.2015.7125186.

[31] A. Kawousi, B. Vahidi, R. Salehi, M. K. Bakhshizadeh, N. Farokhina, and S. H. Fathi, "Application of the Bee algorithm for selective harmonic elimination strategy in multilevel inverters," *IEEE Trans. Power Electron.*, vol. 27, no. 4, pp. 1689–1696, Apr. 2012, doi: 10.1109/TPEL.2011.2166124.

[32] R. N. Ray, D. Chatterjee, and S. K. Goswami, "An application of PSO technique for harmonic elimination in a PWM inverter," *Appl. Soft Comput.*, vol. 9, pp. 1315–1320, 2009, doi: 10.1016/j.asoc.2009.05.002.

[33] B. Makhlouf, O. Bouchhida, and M. Nibouche, "Design, analysis and implementation of real-time harmonics elimination: A generalised approach," *IET Power Electron.*, vol. 7, no. 9, pp. 2424–2436, 2014, doi: 10.1049/iet-pel.2013.0687.

[34] J. R. Wells, X. Geng, P. L. Chapman, P. T. Krein, and B. M. Nee, "Modulation-based harmonic elimination," *IEEE Trans. Power Electron.*, vol. 22, no. 1, pp. 336–340, Jan. 2007, doi: 10.1109/TPEL.2006.888910.

[35] A. Tripathi and G. Narayanan, "Torque ripple minimization in neutral-point-clamped three-level inverter fed induction motor drives operated at low-switching-frequency," *IEEE Trans. Ind. Appl.*, vol. 52, no. 2, pp. 1477–1488, Mar./Apr. 2016, doi: 10.1109/SPEEDAM.2016.7525855.

Marcin Steczek (M'16) was born in Lodz, Poland, in 1981. He received the M.Sc.Eng. degree in networks and power systems in 2005 from Łodz University of Technology, Lodz, Poland, and the Ph.D. degree in electrical engineering from Warsaw University of Technology, Warsaw, Poland, in 2012.

From 2005 to 2012, he was an Assistant and since 2013 he has been an Assistant Professor in the Institute of Electrical Power Engineering, Lodz University of Technology. His research interests include compatibility in dc electric traction systems, methods of determination of traction vehicle input impedance, and disturbing influence of inverter traction drive systems on railway signaling and control system.

Dr. Steczek has been a member of the Association of Polish Electrical Engineers, Department in Lodz, since 2005.

Piotr Chudzik received the M.Sc. (Tech.) degree in electrical engineering and the Ph.D. degree in control engineering from Lodz University of Technology, Lodz, Poland, in 1993 and 2003, respectively.

He joined the Institute of Automatic Control, Lodz University of Technology, in 1993 and is currently a Lecturer. Since 2011, he has been with Enika Lodz, Lodz, Poland, as a Design Engineer. He designs power converter control systems and drives for trams, trolleybuses, and E-buses. He has participated in a number of research projects. His research interests include power electronics and motor drives. He is also a Consultant to industry in the areas mentioned above.

Adam Szeląg received the M.Sc., Ph.D., and D.Sc. degrees in electrical engineering from Warsaw University of Technology, Warsaw, Poland, in 1982, 1990, and 2003, respectively.

He is currently a Professor in the Electrical Engineering Department Electric Traction Division, Warsaw University of Technology. He is the coauthor of three applied patents and new technical solutions implemented in electric mass transport. He is the author/coauthor of many papers, four student handbooks, four research monographs, and has been a Supervisor of four completed Ph.D. theses. His research interests include electric traction systems power supply, modeling and simulation, energy quality, and EMC.

Prof. Szeląg is the Chairman of the Electric Traction Section of the Electrotechnical Committee of the Polish Academy of Sciences, a member of the Institution of engineering and Technology, U.K., the Association of Polish Electrical Engineers SEP, as well as the Scientific and Technical Council of Warsaw Metro and Institute of Electrotechnical Engineering.